Mon. Not. R. astr. Soc. (1969) **145**, 249–269.

GRAIN TEMPERATURES IN INTERSTELLAR DUST CLOUDS

Michael W. Werner and E. E. Salpeter

(Received 1969 June 16)

SUMMARY

We have solved in detail the problem of radiative transfer in a spherical dust cloud, including the effects of scattering and of reradiation by the grains. The results have been used to calculate the grain temperature as a function of position in such a cloud, and to estimate such quantities as the cloud albedo and the radiant energy density in a cloud.

Several grain models have been considered, including cases in which the far infra-red emissivity is enhanced by impurity oscillators. It is shown that the near infra-red component of the interstellar radiation field keeps the central grain temperatures from declining rapidly within clouds of moderate opacity. For very opaque clouds ($\tau_0 > 100$), a limiting central grain temperature greater than $2{\cdot}7\,^{\circ}\mathrm{K}$ is set by the thermal radiation of the outer grains. The results indicate that grains of the types considered are not able to become sufficiently cold ($T \lesssim 4\,^{\circ}\mathrm{K}$) in the dust clouds commonly observed in the Galaxy to permit the formation of solid H_2 mantles.

1. INTRODUCTION

The temperature of dust grains in interstellar space is of interest for a number of reasons. Molecules are known to exist in interstellar space, and fairly low temperatures are probably required for their formation on the surface of grains. The possible formation of mantles of solid H_2 around grain cores has been suggested recently (Wickramasinghe & Reddish 1968) and this would require particularly low grain temperatures, $T_g \lesssim 4\,^{\circ}\mathrm{K}$. Since gas–grain collisions may be an important cooling mechanism, the grain temperature in dense clouds could have an influence on the evolution of the clouds. One might hope to find particularly low values of T_g in the interiors of opaque dust clouds. The aim of the present paper is the calculation of T_g for a number of different types of grains as a function of optical depth inside a cloud.

The temperature, T_g, of a spherical grain of radius a is determined by the heat-balance equation

$$\int F(\lambda)Q(\lambda)\,d\lambda = \int B(\lambda, T_g)Q(\lambda)\,d\lambda \qquad (1)$$

where B is the Planck function (in erg $\mathrm{cm^{-2}\text{-}s^{-1}\text{-}sr^{-1}\text{-}\mu^{-1}}$) for blackbody radiation at temperature T_g and $F(\lambda)$ is the radiation flux (in the same units) incident on the grain in the form of diffuse starlight and/or radiation from other grains. $Q(\lambda)$ is the absorption efficiency (ratio of absorption cross-section to geometric cross-section, πa^2) of the grain as a function of wavelength λ. Since $F(\lambda)$ never approaches a true blackbody radiation field in interstellar space, the two integrals

in equation (1) generally refer to different wavelength regions. For grains in free space or in clouds of moderate opacity, ultra-violet, visible, and near infra-red wavelengths dominate on the left-hand side of equation (1), but T_g is always so low that the right-hand integral covers wavelengths in the far infra-red. In general, then, it is the slope of Q as a function of λ, and not the absolute value of Q, which is the crucial factor in determining the value of T_g. In Section 2 we describe the choices for $Q(\lambda)$ we shall explore, including those appropriate for (a) pure graphite grains, (b) grains with a graphite core and an ice-mantle and (c) some examples where $Q(\lambda)$ is enhanced in the far infra-red to simulate the possible effects of impurity oscillators. The chosen mean interstellar radiation field is also given in Section 2. Although grains may be heated by processes other than the absorption of radiation, radiative heating is by far the most important mechanism. Other heating processes are discussed in Section 5e.

The actual radiation flux $F(\lambda)$ inside an interstellar cloud has a component at near infra-red and shorter wavelengths determined by absorption and scattering of the incident starlight and a far infra-red component determined by radiation emitted by dust grains. We shall calculate T_g explicitly for spherical dust clouds of uniform density for various values of the visual optical depth τ (at $\lambda = 0{\cdot}55\ \mu$) from the position of the grain to the cloud surface. A range of values for the total visual optical depth to the centre, τ_0, will be considered. The highest value of τ_0 reported for dust clouds in the Galaxy is of the order of 5 (Heiles 1968), but higher opacities would be difficult to measure. Since we wish to include cases with fairly large values of τ and τ_0 (τ_0 up to ~ 100, say) the problem of radiative transfer in the cloud has to be solved in some detail. We shall simplify the numerical work greatly by treating the scattering of the incident starlight in an approximate manner and neglecting attenuation in the cloud of the infra-red radiation emitted by grains. This approximation is justified even if τ_0 is large in the visible, because $Q(\lambda)$ is extremely small in the far infra-red, so that the cloud is transparent to grain radiation as long as $\tau_0 \ll 10^3$. We discuss our treatment of the radiative transfer problem in Section 3 and in the Appendix. The results of the calculation are presented and discussed in Section 4, and their sensitivity to the adopted parameters is discussed in Section 5. Our conclusions are summarized in Section 6.

2. INTERSTELLAR RADIATION FIELD AND TYPES OF GRAINS

(a) *Radiation field*

Let $F_0(\lambda)$ be the mean flux of diluted starlight in 'normal' interstellar space (as distinct from the interior of a dense cloud) in the galactic plane in the general vicinity of the sun. Recent night-sky measurements by Lillie (1968) give estimates for the flux and the colour-temperature in the ultra-violet and visible ($\lambda \gtrsim 0{\cdot}21\mu$), and agree well with the theoretical ultra-violet flux estimated by Habing (1968). We represent $F(\lambda)$ as the sum of three dilute blackbody spectra,

$$F(\lambda) = \sum_i W_i B(\lambda, T_i) \qquad (2)$$

with T_i and W_i as shown below.

TABLE I

Interstellar radiation field

T_i	14500	7500	4000
W_i	4×10^{-16}	$1\cdot5\times10^{-14}$	$1\cdot5\times10^{-13}$

Equation (2) reproduces Lillie's colour-temperatures in the ultra-violet and visible and Lambrecht & Zimmermann's (1954) colour-temperature in the red ($\lambda\gtrsim0\cdot8\,\mu$) and also gives the usual value for the equivalent energy density temperature T_{eq},

$$T_{eq}=\left(\sum_i W_iT_i^4\right)^{1/4}=3\cdot2\,^\circ\mathrm{K}. \tag{3}$$

Our equation (2) is probably still fairly reliable in the near infra-red, $\lambda\sim1$ to 2μ, but it might be an underestimate for the unexplored region of slightly longer wavelengths. We have also added to $F_0(\lambda)$ in all our numerical calculations the isotropic microwave background radiation, i.e. undiluted blackbody radiation at $2\cdot7\,^\circ$K. This radiation prevents T_g from falling below $2\cdot7\,^\circ$K under any circumstances. In the interior of a cloud we shall include radiation from grains *inside* the cloud (see Section 3c), but we have neglected radiation from other grains in the galactic disc. The sensitivity of our results to changes in F_0 is discussed in Section 5b.

(b) *Grain models*

Many suggestions have been made concerning the nature of interstellar grains, each leading to a different shape for Q as a function of λ and hence to a different value of T_{go}, the grain temperature in 'normal' interstellar space. From the various possibilities without any impurity oscillators we chose two: (a) pure spherical graphite grains of radius $a=0\cdot05\mu$ and (b) a graphite core of radius $0\cdot05\mu$ surrounded by a 'dirty-ice' mantle of outer radius $a=0\cdot15\mu$. Case (a) gives a larger value for T_{go} of $\sim40\,^\circ$K than most types of grains. Such grains may be produced in the atmospheres of carbon stars, and subsequently expelled into the interstellar medium (Hoyle & Wickramasinghe 1962). Case (b) gives a lower value than most, $T_{go}\sim15\,^\circ$K, and such core-mantle (CM) grains fit the observed optical extinction curves fairly well.

For each type of grain we need to evaluate $Q(\lambda)$, the efficiency for true absorption, the scattering efficiency $Q_s(\lambda)$ (total scattering cross-section divided by πa^2) and the asymmetry parameter $g(\lambda)$ of the scattering function. The evaluation of Q, Q_s and g from the complex refractive index $m=n-ik$ at 'optical' wavelengths (ultra-violet to near infra-red) requires the exact Mie theory, as discussed by van de Hulst (1957) and Wickramasinghe (1967). For graphite m as a function of λ has been measured by Taft & Phillipp (1965) and the optical parameters have been calculated with a computer program kindly provided by Dr N. C. Wickramasinghe. For the CM grains, the optical parameters were provided by Dr K. S. Krishna Swamy. The 'dirty-ice' mantle was assumed to have an index of refraction $m=1\cdot33-0\cdot05i$ in the visible region. In the ultra-violet, the effects of the absorption bands of H_2O, NH_3, and CH_4 were included in the mantle refractive index, as suggested by Field, Partridge & Sobel (1967). The calculated values for g, for the extinction efficiency $Q_T(\lambda)=Q(\lambda)+Q_s(\lambda)$, and for the albedo, $Q_s(\lambda)/Q_T(\lambda)$, are given in Table II for representative wavelengths.

TABLE II

Optical properties of grains

	Graphite grains, $a = 0{\cdot}05\mu$.		Core-mantle grains, $a = 0{\cdot}15\mu$		
$\lambda(\mu)$	Q_T	A	Q_T*	A*	g
0·1	2·79	0·50	2·39	0·524	0·5
0·15	1·12	0·20	2·60	0·498	0·455
0·2	3·00	0·44	3·27	0·744	0·415
0·25	3·40	0·60	2·54	0·698	0·37
0·3	3·30	0·48	2·07	0·664	0·36
0·35	2·82	0·40	1·80	0·627	0·385
0·4	2·20	0·34	1·60	0·609	0·385
0·45	1·75	0·29	1·41	0·591	0·365
0·5	1·41	0·25	1·22	0·573	0·34
0·55	1·00	0·20	1·05	0·556	0·305
0·6	0·93	0·18	0·905	0·540	0·265
0·65	0·75	0·15	0·787	0·521	0·220
0·7	0·69	0·13	0·685	0·499	0·190
0·75	0·60	0·11	0·598	0·473	0·165
0·8	0·49	0·09	0·524	0·447	0·14
0·85	0·47	0·08	0·460	0·420	0·12
0·9	0·42	0·08	0·406	0·392	0·105
1·03	0·341	0·0609	0·245	0·183	0·07
1·55	0·111	0·000	0·067	0·091	0·045
2·07	0·071	0·000	0·031	0·03	0·02
3·10	0·039	0·000	0·013	0·00	0·00
4·13	0·024	0·000	0·003	0·00	0·00

Q_T = total extinction efficiency; A = albedo; g = asymmetry parameter of scattering function. $g = 0$ has been assumed for graphite. * These data for $\lambda \leq 0{\cdot}9\mu$ are based on the work of Krishna Swamy (1969, to be published): see also Donn & Krishna Swamy (1969). Other values were calculated with programmes provided by Dr N. C. Wickramasinghe.

To simplify our treatment of the scattering problem, we have replaced the actual scattering function by a fraction $(1-g)$ of isotropic scattering plus g of forward scattering (i.e. no scattering at all). We then adopt for the effective extinction efficiency $Q_E(\lambda)$ and the effective albedo $\gamma(\lambda)$, the values

$$Q_E(\lambda) = Q(\lambda)+[1-g(\lambda)]Q_s(\lambda); \qquad \gamma(\lambda) = [1-g(\lambda)]Q_s(\lambda)/Q_E(\lambda). \tag{4}$$

The true optical properties of the grains are given in Table II; equation (4) defines the effective properties which are used in the radiative transfer problem.

Luckily, intermediate wavelengths ($\lambda \sim 10\mu$ to 75μ, say) are quite unimportant for our purposes but we need to know $Q(\lambda)$ in the far infra-red for the grain radiation. For the far infra-red, $\lambda \gg a$, and the following approximation, due to van de Hulst (1957), may be used. Let a be the outer radius of a spherical composite grain and qa the radius of the grain core. For our CM grains $q = 1/3$, and $q = 1$ for pure graphite. Then,

$$Q(\lambda) = \frac{8\pi a}{\lambda} Re\left\{i\,\frac{(\varepsilon_2-1)(\varepsilon_1+2\varepsilon_2)(1-q^3)+3q^3\varepsilon_2(\varepsilon_1-1)}{(\varepsilon_2+2)(\varepsilon_1+2\varepsilon_2)(1-q^3)+3q^3\varepsilon_2(\varepsilon_1+2)}\right\} \tag{5}$$

where $\varepsilon_1 = m_1(\lambda)^2$ and $\varepsilon_2 = m_2(\lambda)^2$ and m_1 and m_2 are the complex refractive indices of the core and mantle, respectively. The data of Taft & Phillipp (1965) give for the far infra-red $m_1 = 6{\cdot}5 - i\,0{\cdot}47\lambda$. For the mantle we take $m_2 = 1{\cdot}73 - 0{\cdot}08i$, based on the work of Bertie & Whalley (1967), and of Irvine & Pollack (1968). This choice of m_2 is strictly correct only for H_2O ice, but other dielectric substances which may be present in the mantle should have a similar refractive index (Greenberg 1968).

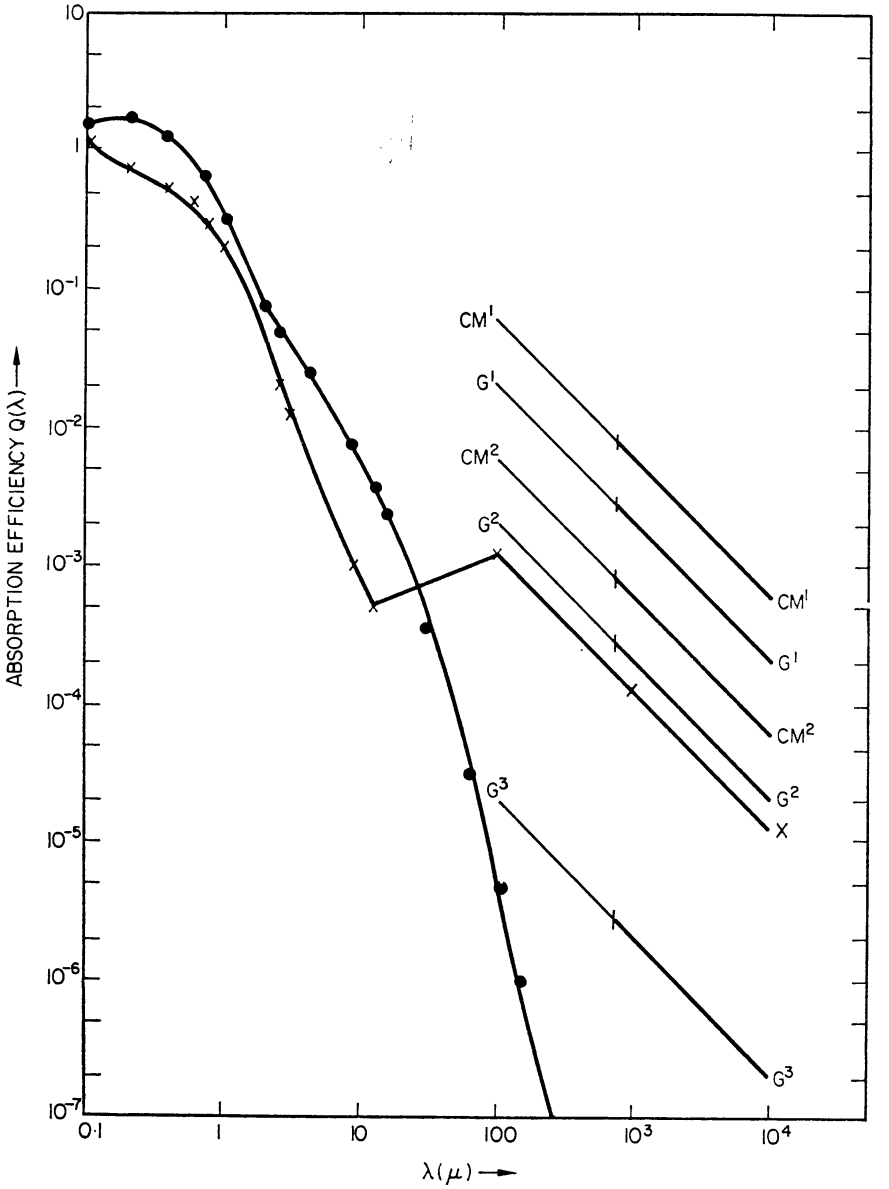

FIG. 1. *Absorption efficiency as a function of wavelength for the grain models studied:* ●—● 0·05μ *pure graphite grains;* ×—× 0·15μ *core-mantle grains. The diagonal lines between* 100μ *and* $10^4\mu$ *show the absorption efficiency for various values of f, the amount of enhancement by impurity oscillators in the far infra-red; f* = 1 *corresponds to the maximum enhancement permitted in the theory of Field* (1969). *CM^1, CM^2; core-mantle grains enhanced with f* = 1, 0·1; *G^1, G^2, G^3: graphite grains enhanced with f* = 1, 0·1, 10^{-3}. *The heavy portions of these curves show the efficiency when the enhancement is effective only at* $\lambda > 750\mu$.

(c) *Inclusion of impurity oscillators*

Hoyle & Wickramasinghe (1967) have argued that grains may contain weakly bound impurity atoms which emit efficiently in the far infra-red and give very much larger values for $Q(\lambda)$ than the classical expression in equation (5). Field (1969) has shown that, for a single impurity mode giving a resonance at an observed frequency ν_1, the integrated absorption efficiency is bounded by

$$\int Q(\lambda)\, d\nu/\nu_1 < 4\pi^2(a/\lambda_1). \tag{6}$$

As a crude model for enhanced efficiency for λ larger than some critical value λ_0 we shall adopt for $Q(\lambda)$ the value

$$Q(\lambda) = f4\pi^2(a/\lambda). \tag{7}$$

Although no limiting theorems are available for distributed resonances, values of f exceeding unity are probably unreasonable. We have carried out calculations, both for graphite and for core-mantle grains, with $f = 1$ and with $f = 0{\cdot}1$ (as well as the orthodox calculations with $f = 0$). We have chosen two values of λ_0 to bracket the extreme cases of interest. (1) $\lambda_0 = 100\mu$, so that the efficiency is enhanced throughout the entire far infra-red region where the grains radiate; and (2) $\lambda_0 = 750\mu$, in which case the enhancement is operative only for extremely low grain temperatures, $T_g \sim 4$°K. We have done an additional case ($f = 10^{-3}$, $\lambda_0 = 100\mu$) for graphite grains; $Q(\lambda)$ is so small for pure graphite grains that even this small impurity contribution will change the grain temperature significantly. An ice-mantle of outer radius $\sim 0{\cdot}05$ of the core radius would produce a similar change in temperature. $Q(\lambda)$ is shown in Fig. 1 for all the cases considered.

3. RADIATIVE TRANSFER IN DUST CLOUDS

We carry out explicit calculations only for spherical dust clouds of uniform internal dust density but show in Section 5a how to generalize our results for other geometries. Let τ_0 be the optical depth for extinction in the visible spectral band, $\lambda = 0{\cdot}55\mu$, from the centre to the outside of the sphere (measured radially). We assume a uniform isotropic flux of diffuse starlight $F_0(\lambda)$, given by equation (2), incident on the outside of the sphere. The physical conditions at some point inside the sphere depend only on the values of τ_0 and of r (see Fig. 2), the fractional radius at which the point is located (and not separately on grain densities and absolute distances). The optical depth for extinction at wavelength λ to the nearest point on the surface from point r, τ_λ, is then

$$\tau_\lambda/\tau = \tau_{0\lambda}/\tau_0 = \frac{Q_E(\lambda)}{Q_V}; \qquad \tau \equiv (1-r)\tau_0. \tag{8}$$

Here τ_0 and τ, which are the variables chosen to define grain position and cloud size, are measured in terms of $Q_V = Q(0{\cdot}55\mu)$, the true extinction efficiency of a single grain to visible light. This is done to facilitate comparison with observed dust clouds. τ_λ and $\tau_{0\lambda}$, however, are the variables entering into the radiative transfer problem; they are thus defined in terms of the modified efficiency of equation (4).

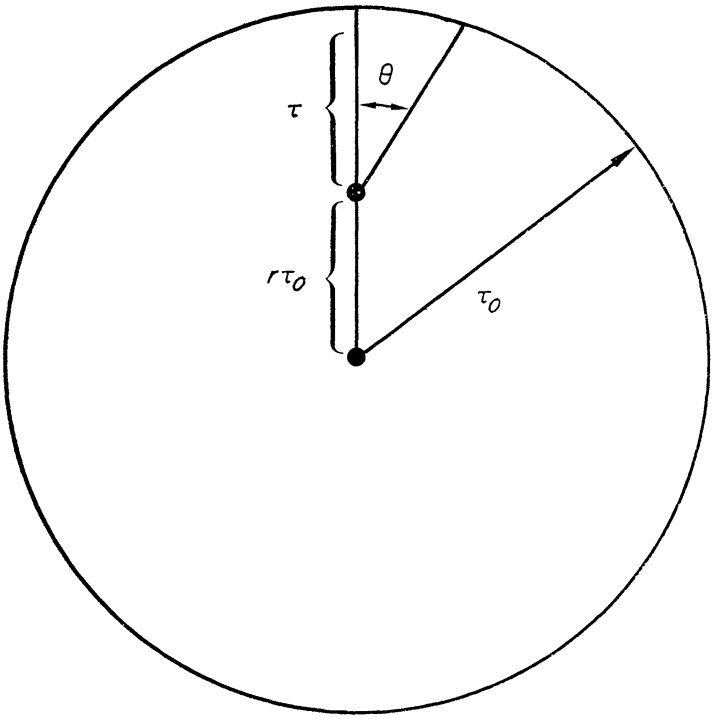

FIG. 2. *Geometry of radiative transfer problem.*

(a) *Attenuated starlight*

To determine the grain-temperature $T_g(\tau)$ at a point r in the cloud from equation (1) we need to determine $F(\lambda, \tau)$, the radiation-flux averaged over directions at this point. F consists (in addition to the constant microwave background $F_{2.7}$) of three contributions, the attenuated unscattered starlight flux F_a, the scattered (without change of wavelength) flux F_s and the flux F_T due to thermal radiation emitted by the grains in the outer layers of the spherical cloud. With μ the cosine of the angle θ shown in Fig. 2, the attenuated flux F_a is

$$F_a(\lambda, \tau) = \tfrac{1}{2}F_0(\lambda)\int_{-1}^{1} d\mu \exp\{\tau_{0\lambda}[-r\mu+(r^2\mu^2-r^2+1)^{1/2}]\} \qquad (9)$$

with $\tau_{0\lambda}$ given by equation (8). The exact value of the integral depends separately on $\tau_{0\lambda}$ and on r, but it can easily be evaluated numerically.

(b) *Scattered starlight*

The exact evaluation of the scattered flux F_s for spherical geometry would be very tedious and would have to be carried out separately for all sets of values of $\gamma(\lambda)$, τ_λ and $\tau_{0\lambda}$. For this reason we adopt an approximate procedure. Consider first cases for which $\tau_{0\lambda} \gtrsim r\tau_{0\lambda} \gg 1$. In such cases (no matter whether $\tau_\lambda = (1-r)\tau_{0\lambda}$ is large or small) the relevant surface effects take place near the closest point on the surface and curvature effects can be neglected. The ratio F_s/F_a can then be evaluated ' in plane geometry ', i.e. for the correct value of τ_λ but in the limit of $\tau_{0\lambda} \to \infty$. In the Appendix a function $H(\gamma(\lambda), \tau_\lambda)$ is derived which is an analytic approximation to the ratio F_s/F_a in a semi-infinite medium at distance τ_λ from

the plane surface with γ the effective albedo in equation (4). The approximation for the spherical case which we shall adopt is

$$F_s(\lambda, \tau) = F_a(\lambda, \tau)\mathrm{H}(\gamma'(\lambda), \tau_\lambda)$$
$$\gamma'(\lambda) = (1-e^{-2\tau_{o\lambda}})\gamma(\lambda) \qquad (10)$$

with $F_a(\lambda, \tau)$ given by equation (9).

The rationale for this procedure is the following. If $\tau_{o\lambda} \gg 1$, γ' reduces to γ and our approximation is accurate, as discussed above (except near the centre of the sphere, but because γ is small we shall not be interested in F_a and F_s for very large values of τ_λ). In the opposite extreme of $\tau_{o\lambda} \ll 1$ only single scattering need be considered and the correct F_s is given by equation (10) with $\gamma' \to 2\tau_{o\lambda}\gamma$. For intermediate values of $\tau_{o\lambda} \sim 1$ equation (10) is merely a convenient interpolation formula, but it is at least of the correct order of magnitude.

(c) *Thermal radiation from outer grains*

In the deep interior of a dense cloud which is very opaque to the incident radiation, $\tau_o \gg 1$, the remaining starlight flux (F_a+F_s) given by equations (9) and (10) is very small and we have to consider the flux F_T of thermal emission from grains in the cloud. F_T depends on the grain temperatures which, in turn, depend on F_T, so that an iterative procedure seems necessary. We are, nevertheless, able to calculate F_T accurately and simply with only a mild restriction for the following reason. Much of the starlight is in the visible and ultra-violet where the absorption efficiency Q is of order unity, whereas the radiation from the grains is in the far infra-red ($\lambda > 75\mu$) where $Q(\lambda)$ is extremely small (see Fig. 1). While allowing clouds with $\tau_o \gg 1$ we can easily restrict ourselves to cases where $\tau_{o\lambda} \sim Q(\lambda)\tau_o \ll 1$ in the far infra-red. In calculating the contribution to the flux F_T at one part of the cloud from radiation emitted by grains in another part, we can then neglect absorption and scattering in the intervening medium entirely. A further simplification is the following: when τ_o is large, most of the thermal radiation comes from the outer layers of the cloud where $\tau \lesssim 1$ and the total energy density of starlight is still comparable with that of thermal radiation. Since the flux is multiplied by $Q(\lambda)$ on the left-hand side of equation (1), the contribution of F_T in the determination of T_g is quite negligible for $\tau \lesssim 1$ or 2, and the following two-step procedure suffices. We calculate a first approximation $T_g^{(1)}$ to the grain temperature at various τ from equation (1) with F replaced by $F_a+F_s+F_{2.7}$. We next evaluate the emission from the grains and hence F_T (see below) using $T_g^{(1)}$ for the grain temperature. We then find final values $T_g(\tau)$ from equation (1) by substituting on the left-hand side

$$F = F_a+F_s+F_T+F_{2.7}. \qquad (11)$$

T_g differs from $T_g^{(1)}$ appreciably only for grains in the deep interior of a dense cloud. These cooler grains contribute little to the total grain radiation, so that further iteration is unnecessary.

Let dF_T be the contribution to F_T at fractional radius r from the centre due to emission from grains in a thin spherical shell at fractional radius rD $(D > 1)$

with volume emissivity ϵ_λ and thickness dt. Evaluation of the angular integration gives

$$dF_T = \frac{1}{2}\, dt \epsilon_\lambda D \log_e \frac{D+1}{D-1}. \tag{12}$$

Now

$$\epsilon_\lambda dt = 4\pi a^2 B(\lambda, T_g^{(1)}(\tau)) \frac{Q(\lambda)}{Q_V}\, d\tau$$

where $T_g^{(1)}(\tau)$ is the grain temperature in the emitting shell (located at position τ). Our final result for the direction-averaged thermal radiation is, then,

$$\left.\begin{aligned} F_T(\lambda, \tau) &= 2\pi a^2 \frac{Q(\lambda)}{Q_V} \int_0^\tau d\tau' B(\lambda, T_g^{(1)}(\tau'))\eta(\tau'); \\ \eta(\tau') &= \frac{\tau_0 - \tau'}{\tau_0 - \tau} \log_e \frac{2\tau_0 - \tau - \tau'}{\tau - \tau'}. \end{aligned}\right\} \tag{13}$$

In equation (13) we have neglected the contribution from shells inside of τ for the reasons stated above.

At the centre of the cloud, $\tau = \tau_0$, the factor η reduces to 2 for all τ'. As discussed above, the main contribution to the integral in equation (13) comes from small τ where the grains are hottest. The temperatures of these exterior grains are independent of τ_0. As $\tau_0 \to \infty$ $F_s + F_a$ tends to zero, but this integral evaluated at $\tau = \tau_0$ goes to a finite limit. Hence, F_T approaches a constant value independent of τ_0 as τ_0 increases in our approximation (cloud still transparent in the far infra-red). Consequently, the central grain temperature, $T_g(\tau_0)$, approaches a limiting value $T_{\rm lim} > 2{\cdot}7\,^\circ$K.

4. RESULTS AND DISCUSSION

(a) *Pure grains*

The calculations described above were carried out numerically on the IBM 360–44 computer at the Institute of Theoretical Astronomy. A grid of optical depth points was used spaced at $\Delta\tau = 0{\cdot}125$ for $\tau \lesssim 4$ and $\Delta\tau = 0{\cdot}5$ for $\tau > 4$. For the graphite grains the range $\tau > 4$ contributed little to the integral in equation (13) and its contribution was omitted. Grain temperatures were determined from equation (1) to the nearest $0{\cdot}05\,^\circ$K.

For graphite and core-mantle grains without impurities a series of computations were carried out for various values of τ_0, the optical depth (at $\lambda = 0{\cdot}55\mu$) to the centre of the spherical cloud. Our main results for the grain temperature $T_g(\tau, \tau_0)$ at a position τ (optical depth from some point inside the cloud to the nearest point on the surface) within a cloud of central opacity τ_0 are plotted in Figs 3 and 4. Also displayed is the locus of points with $\tau = \tau_0$, i.e. the temperature at the centre of the cloud, $T_g(\tau_0)$. The values for $\tau_0 = 0$, the free-space grain temperature, were $T_{go} = 43{\cdot}1\,^\circ$K for graphite and $16{\cdot}85\,^\circ$K for core-mantle grains. These values agree well with the free-space temperatures calculated by Krishna Swamy & Wickramasinghe (1968). The limiting values set by the effects of F_T for $T_g(\tau_0)$ as $\tau_0 \to \infty$ in our approximation were $T_{\rm lim} = 11{\cdot}05\,^\circ$K for graphite and $3{\cdot}50\,^\circ$K for CM grams. These values are approached only for exceedingly high τ_0.

Note that $T_g(\tau, \tau_0)$ at a given τ decreases slightly with increasing τ_0 when τ_0 is fairly small, because of increased shielding of the starlight from the opposite hemisphere; the results become independent of τ_0 for large τ_0 because this shielding is then essentially complete. $T_g(\tau, \tau_0)$ as a function of τ for large τ_0 decreases fairly rapidly at first from $\tau = 0$ to $\tau \sim 2$ or 3, as expected. A striking feature of our results, however, is the surprisingly slow decrease of $T_g(\tau, \tau_0)$ for larger values of τ, e.g. from $\tau = 3$ to 30, and the related slow decrease of $T_g(\tau_0)$ with τ_0. This arises

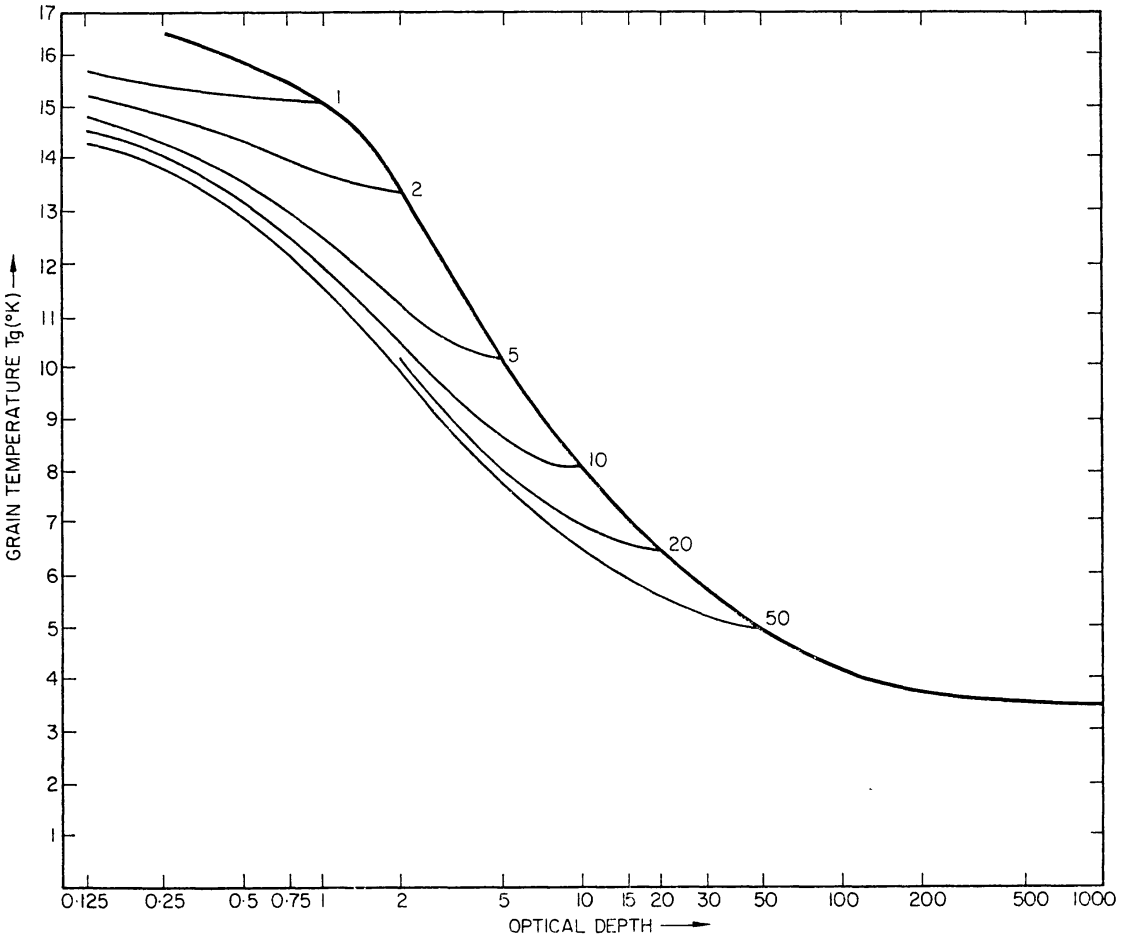

FIG. 3. *Temperatures for 0·15μ radius core-mantle grains without impurities inside spherical interstellar dust clouds. The heavy line shows the temperature at the centre of a cloud with optical depth τ at $\lambda = 5500$ Å. The thin curves show grain temperature as a function of optical depth within a cloud the total opacity of which is indicated by the number on the right-hand end of the curve.*

from the rapid decrease of $Q_E(\lambda)$ from the visible to the near infra-red, and from the fact that the dilute starlight radiation field of equation (2) contains an appreciable amount of energy in the near infra-red ($\lambda \sim 1$ to 3μ). This infra-red component of the starlight is thus able to filter into the interior even of a very thick cloud. For example, a 'thick' cloud with $\tau_0 \sim 30$ is still optically thin ($\tau_{0\lambda} \lesssim 1$) at $\lambda \gtrsim 2\mu$. The efficacy of this small amount of starlight in keeping T_g from falling is aided by the fact that the total amount of thermal energy emitted by a grain varies very steeply with $T(\propto T^5 - T^7)$ for small T, as shown in Section 5b. A

relatively large change in $F_0(\lambda)$ is thus necessary to produce a small change in T_g.

For $\tau_0 > 100$ the penetration of starlight finally becomes unimportant and T_g approaches the values $T_{\rm lim}$ described above. In this limit the heating comes only from the grain radiation from the outer layers of the cloud (plus the microwave background) and the large value of $T_{\rm lim}$ for the pure graphite grains may seem

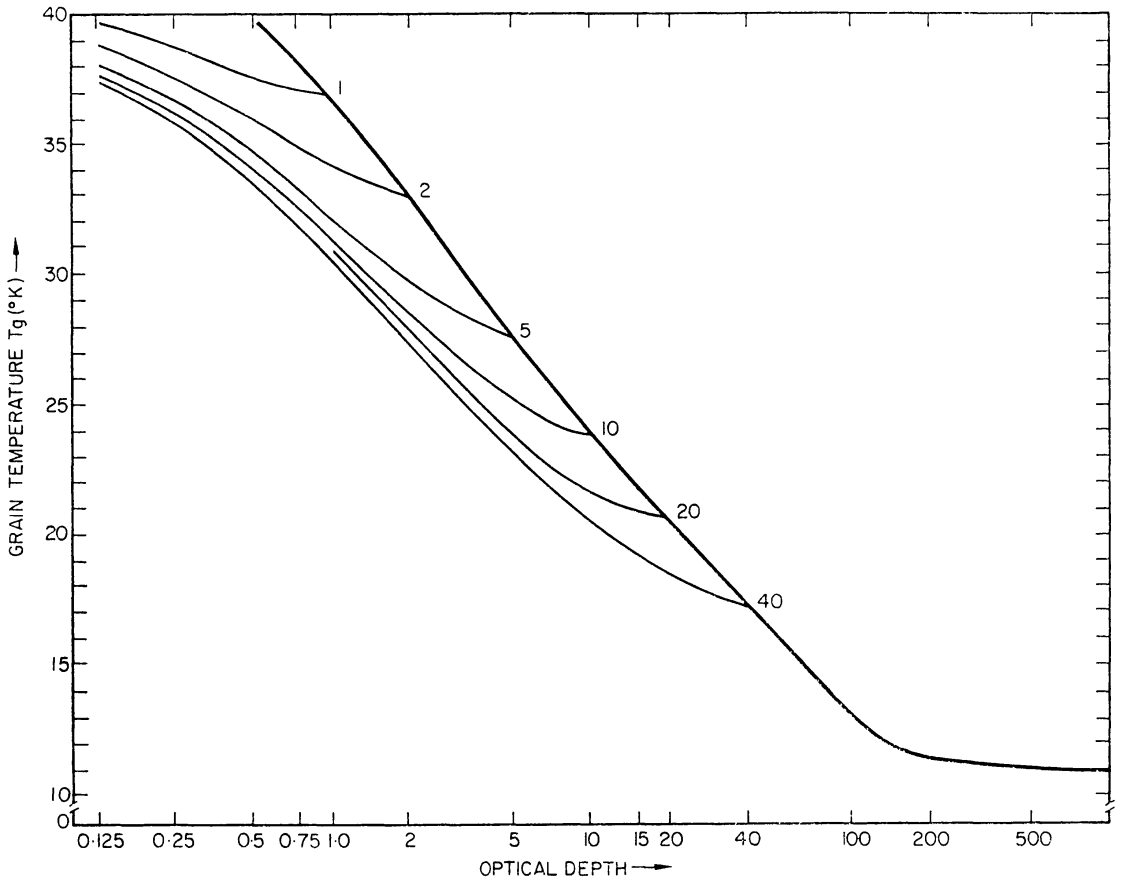

FIG. 4. *Temperatures for 0·05μ radius graphite grains without impurities inside spherical interstellar dust clouds. The heavy line shows the temperature at the centre of a cloud with optical depth τ at $\lambda = 5500$ Å. The thin curves show grain temperature as a function of optical depth within a cloud the total opacity of which is indicated by the number of the right-hand end of the curve.*

surprising. This large value of $T_{\rm lim}$ results from the fact that the outer grains are appreciably hotter than the energy density temperature $T_{eq} \sim 3$ °K and that $Q(\lambda)$ continues to decrease with increasing λ in the far infra-red for graphite grains (see Fig. 1); so there is still a 'greenhouse effect' leading to $T_{\rm lim} > T_{eq}$.

(b) *Effects of impurities*

As described in Section 2 we have also explored the effects of enhanced absorption efficiency in the far infra-red, both for graphite and for CM grains. T_{go} and $T_{\rm lim}$ are tabulated below for all cases considered. For two representative cases, $\tau_0 = 5$ and $\tau_0 = 30$, we have carried out numerical computations for all examples of grain types. The results for T_g as a function of τ are given in Fig. 5

TABLE III

Extreme temperatures for various grain models

Type of grain	$\lambda_0(\mu)$	f	T_{go} (°K)	$T_{\rm lim}$ (°K)
Pure graphite			43·1	11·05
Impure graphite	100	1	11·015	3·35
Impure graphite	100	0·1	17·454	3·55
Impure graphite	100	10^{-3}	43·1	4·15
Impure graphite	750	1	43·1	3·15
Impure graphite	750	0·1	43·1	3·0
Pure core-mantle			16·85	3·5
Impure core-mantle	100	1	7·796	3·39
Impure core-mantle	100	0·1	12·345	3·26
Impure core-mantle	750	1	15·25	3·10
Impure core-mantle	750	0·1	16·75	3·05

T_{go} = free-space temperature. $T_{\rm lim}$ = limiting central temperature in cloud of very high optical depth.

for CM and in Fig. 6 for graphite grains. The inclusion of strong enhancement at all far infra-red wavelengths ($\lambda_0 = 100\mu$) lowers T_g uniformly throughout the cloud and produces similar values of T_g for the graphite and the CM grains. If $\lambda_0 = 750\mu$, T_{go} is not strongly affected, but for strong enhancement ($f = 1$),

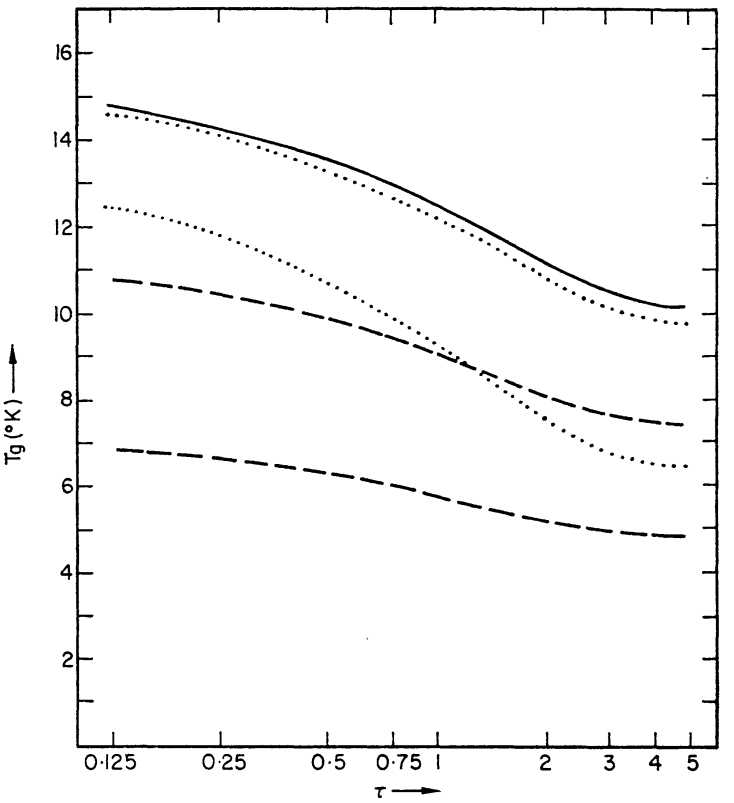

FIG. 5a. *Variation of temperature with position in a dust cloud with $\tau_0 = 5$ at $\lambda = 5500$ Å for $a = 0{\cdot}15\mu$ radius core-mantle grains using various models for the far infra-red absorption efficiency. The absorption efficiency is raised to a value $Q(\lambda) = f4\pi^2 a/\lambda$ for $\lambda > \lambda_0$. $f = 1$ corresponds to the maximum enhancement by impurities permitted in the theory of Field* (1969). *Solid curve: no enhancement by impurities ($f = 0$); upper dotted curve: impurities with $f = 0{\cdot}1$, $\lambda_0 = 750\mu$; lower dotted curve: $f = 1{\cdot}0$, $\lambda_0 = 750\mu$; upper dashed curve: $f = 0{\cdot}1$, $\lambda_0 = 100\mu$: lower dashed curve: $f = 1{\cdot}0$, $\lambda_0 = 100\mu$.*

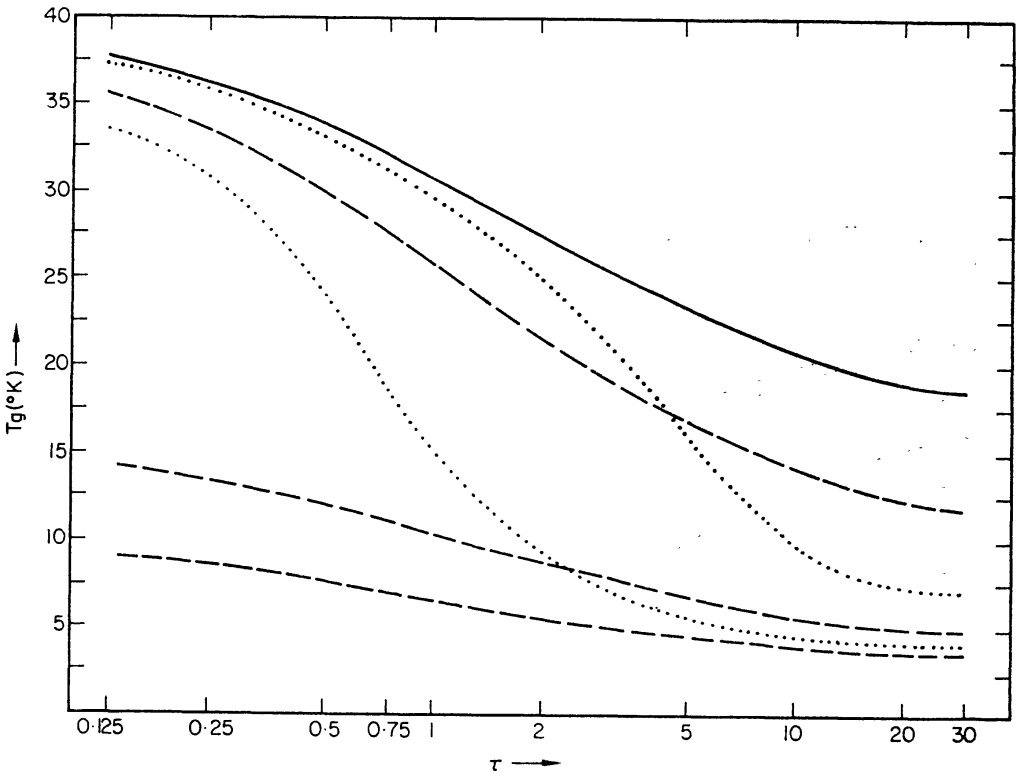

FIG. 5b. *Same as Fig. 5a, for cloud with* $\tau_0 = 30$.

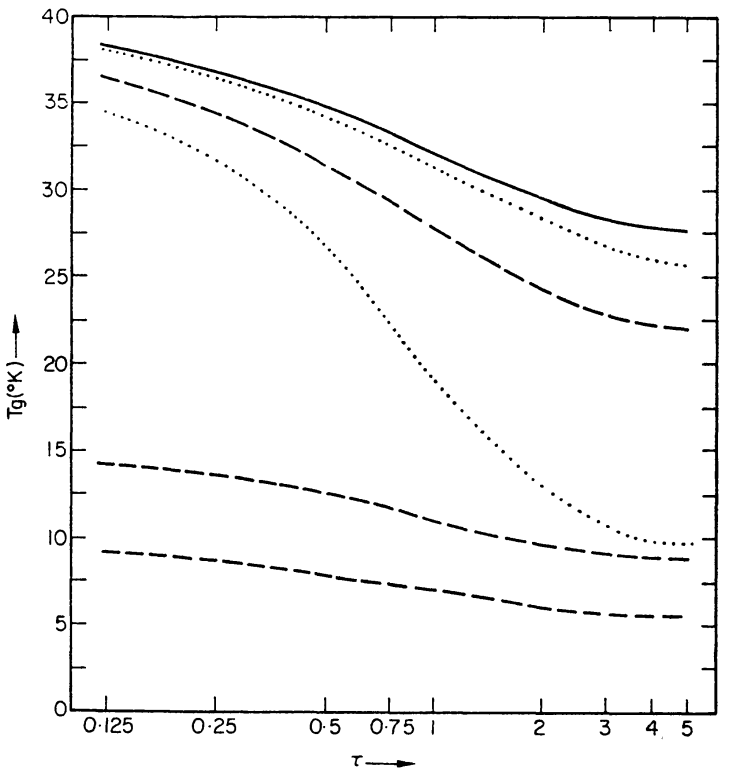

FIG. 6a. *Variation of temperature with position in a dust cloud with* $\tau_0 = 5$ *at* $\lambda = 5500$ *Å for* $a = 0{\cdot}05\mu$ *radius graphite grains using various models for the far infra-red absorption efficiency. The absorption efficiency is raised to a value* $Q(\lambda) = f4\pi^2 a/\lambda$ *for* $\lambda > \lambda_0$. $f = 1$ *corresponds to the maximum enhancement by impurities permitted in the theory of Field* (1969). *Solid curve: no enhancement* ($f = 0$); *upper dotted curve: impurities with* $f = 0{\cdot}1$, $\lambda_0 = 750\mu$; *lower dotted curve:* $f = 1{\cdot}0$, $\lambda_0 = 750\mu$; *upper dashed curve:* $f = 10^{-3}$, $\lambda_0 = 100\mu$; *middle dashed curve:* $f = 0{\cdot}1$, $\lambda_0 = 100\mu$; *lower dashed curve:* $f = 1{\cdot}0$, $\lambda_0 = 100\mu$.

for moderate and large τ the temperatures depend very little on the exact value of λ_0, since the temperature is approaching 4 °K in both cases. The value of λ_0 does affect the temperature profile of the cloud. Note that for $\tau_0 = 5$, corresponding to the most opaque clouds observed in the Galaxy, the temperature in no case falls below ~ 5 °K.

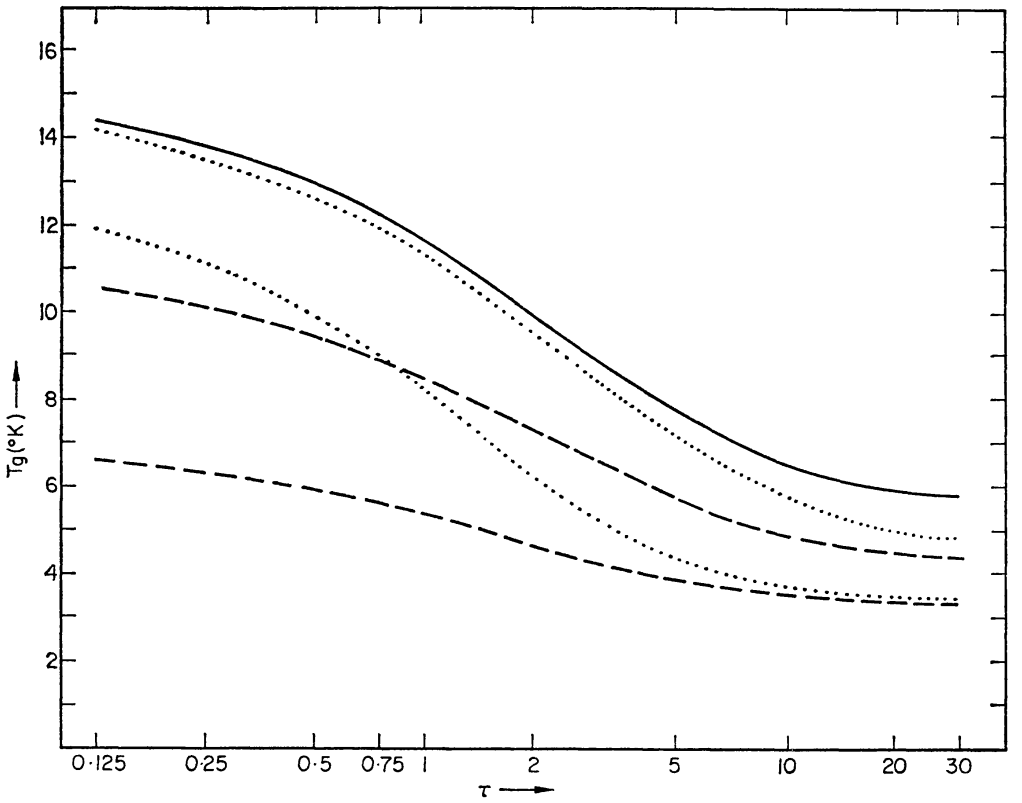

FIG. 6b. *Same as Fig. 6a, for cloud with* $\tau_0 = 30$.

For $f = 1$, we see that $T_g(\tau_0)$ approaches $T_{\lim}$ even for τ_0 as low as 30. The enhancement of $Q(\lambda)$ in the far infra-red has a particularly strong influence on processes involving the thermal radiation of the grains because $Q(\lambda)$ enters quadratically in the term involving $F_T(\lambda)$ on the left-hand side of equation (1) (cf. equation (13)). This explains the interesting result that the lowest values of $T_{\lim}$ are reached for the case $f = 0{\cdot}1$, $\lambda_0 = 750\mu$ (see Table III). Such a grain can become colder than one with $f = 1$ even though it radiates less efficiently, because it absorbs much less thermal radiation from the outer grains.

(c) *Energy absorbed*

In Fig. 7, we have plotted E_A, the energy absorbed by a grain per unit surface area, as a function of τ for $\tau_0 = 30$, and for choices of $Q(\lambda)$ in the far infra-red giving extreme values for this quantity for each of the two types of grains. For small τ, E_A is independent of grain type and of $Q(\lambda)$. For larger τ, the influence of the thermal radiation from the exterior grains and of the microwave background is clearly evident and produces significantly higher values of E_A for the cases with enhanced $Q(\lambda)$. The free-space value of E_A are $4{\cdot}65 \times 10^{-3}$ erg cm^{-2} s^{-1} for graphite, and $2{\cdot}48 \times 10^{-3}$ erg cm^{-2} s^{-1} for the CM grains.

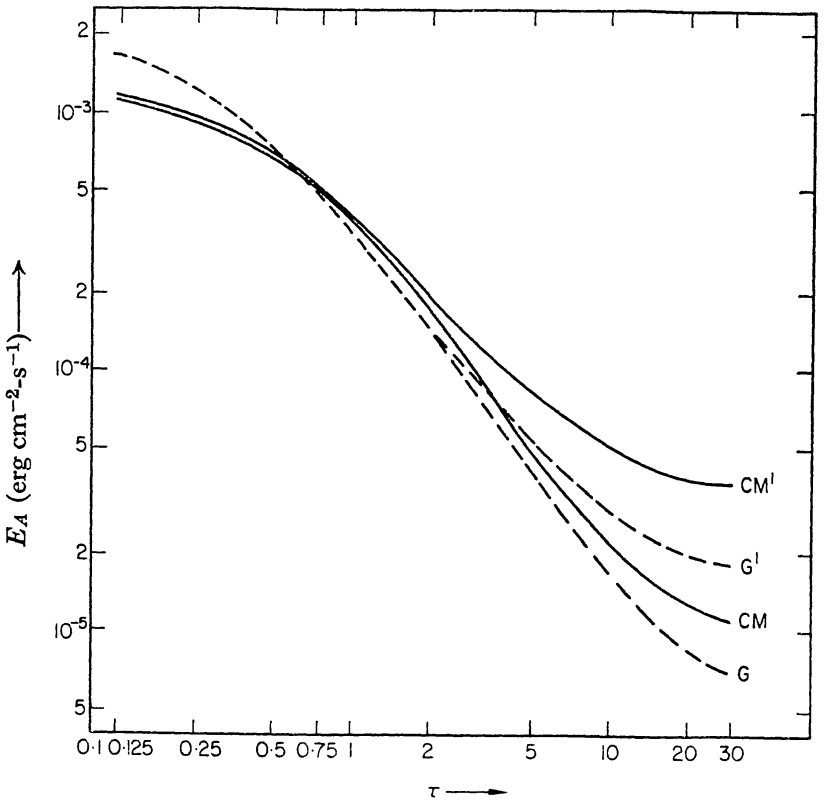

FIG. 7. *E_A, energy absorbed by a grain per square centimetre surface area per second, for graphite and core-mantle grains as a function of position in a cloud of optical depth $\tau = 30$ at $\lambda = 5500$ Å. Curves CM, G: core-mantle and graphite grains with no impurity enhancement of the far infra-red absorption efficiency; Curves CM¹-, G¹-grains with maximum impurity enhancement throughout the far infra-red.*

(d) *Albedo*

By computing F_s at $\tau = 0$, and comparing it with $F_0(\lambda)$, we have estimated the total albedo of the clouds, defined as A = (energy incident)/(scattered energy escaping). For the graphite grains, $A \sim 7$ per cent, and $A \sim 12$ per cent for CM grains, independent of cloud size. The low value of A indicates that scattering is not very important in the total energy budget of the cloud; however, it must be included in the analyses to provide an accurate determination of T_g for small τ, which in turn determines the spectrum of $F_T(\lambda)$.

(e) *Energy density*

With A defined as above, it can be shown that the total energy density, U_T, of thermal radiation from the outer grains at the centre of a dense cloud is $\frac{1}{4}(1-A)U_0$, where U_0 is the energy density of starlight in free-space. $U_0 \sim 0{\cdot}5$ ev cm^{-3} for our choice of $F_0(\lambda)$. It also follows that the value of U_T at an average position in the interior of such a cloud is $\sim \frac{3}{8}(1-A)U_0$.

Because of the small value of $Q_E(\lambda)$ in the near infra-red, $U_s(\tau_0)$, the energy density of attenuated and scattered starlight at the cloud centre, drops slowly with increasing τ_0. We find that $U_s(\tau_0) \gtrsim \frac{1}{4}U_0$ until τ_0 becomes greater than 5. For $\tau_0 \sim 5$, the thermal radiation density at the cloud centre is comparable to $U_s(\tau_0)$, and the total energy density (excluding the microwave background) is

$\sim 0{\cdot}5\ U_0$. The starlight makes the major contribution to E_A even for $\tau_0 \gg 5$, because $Q(\lambda)$ is so small in the far infra-red.

5. EFFECTS OF VARYING PARAMETERS

(a) *Other geometries*

We have considered only spherically symmetric, constant density dust clouds, but our results should be applicable to other cloud geometries. For a non-uniform spherically symmetric dust cloud the values of $T_g(\tau_0)$ and $T_{\rm lim}$ derived above will still be correct. The temperature profiles (T_g *vs.* τ) of Figs 3 and 4 will also be correct for such non-uniform clouds in those cases (τ_0 not too large) where the thermal radiation from the outer grains is unimportant. Our results can be applied to non-spherical clouds in the following way. Let τ be the optical depth at $\lambda = 0{\cdot}55\mu$ from the grain under consideration to the (optically) nearest point on the surface of the cloud. Let $2\tau'$ be the greatest optical extinction along any line of sight through the cloud. It follows that the temperature T_g of the grain under consideration obeys

$$T_g(\tau_0 = \tau) > T_g > T_g(\tau, \tau')$$

where $T_g(\tau_0 = \tau)$ is the central temperature in a spherical cloud of radius τ and $T_g(\tau, \tau')$ is the temperature at position τ in a cloud of radius τ'.

Tighter limits on T_g are obtainable for non-spherical clouds of regular (e.g. ellipsoidal) geometry. The limits on T_g can be obtained from Figs 3 and 4, so that T_g can easily be determined to within a few degrees.

(b) *Variation of radiation field*

We have investigated the effect on T_g of changes in the incident flux, $F_0(\lambda)$, by a test-computation in which $F_0(\lambda)$ was decreased at all wavelengths by a factor of 2/3. For small or moderate τ the decrease in T_g was ~ 5 per cent for pure graphite, and ~ 8 per cent for CM grains. Thus $F_0(\lambda) \propto T_g{}^{\beta}$ with $\beta \sim 7$ for graphite, and $\beta \sim 5$ for CM grains. For large τ the percentage effect on T_g is even smaller.

Any galactic radiation in the very far infra-red ($\lambda \gtrsim 100\mu$) will penetrate to the central regions of even opaque clouds and will augment the thermal flux $F_T(\lambda)$ there. We have done some test calculations where we have added radiation at $\lambda \sim 100\mu$ with the energy flux measured by Hoffmann & Frederick (1969), which corresponds to an energy output of ~ 3 per cent of the total optical luminosity of the Galaxy. This addition increased the thermal energy absorbed by centrally located grains by up to 25 per cent and increased $T_{\rm lim}$ by up to 6 per cent over the values listed in Table III.

(c) *Clouds of very high opacity*

Thermal radiation from the grains in the outer layers of an opaque cloud becomes important for $\tau_0 \gtrsim 100$ for graphite and CM grains, and at $\tau_0 \gtrsim 30$ for grains with the most effective impurity modes.* We have assumed throughout that the cloud remains optically thin to this thermal radiation. This assumption breaks down when $\tau_0 > \tau_0{}^c$ defined by

$$\tau_0{}^c Q'(\lambda_c) \approx Q_V \sim 1.$$

Here $Q'(\lambda_c)$ is the absorption efficiency at the wavelength where this thermal

* The thermal radiation is therefore not important in ordinary dust clouds.

radiation has its peak. For graphite grains $\lambda_c \sim 75\mu$, $\tau_o^c \sim 5 \times 10^4$; for CM grains $\lambda \sim 200\mu$, $\tau_o^c \sim 1600$; and for grains with efficient impurity modes $\lambda_c \sim 300\mu$, $\tau_o^c \sim 50$. For $\tau_o > \tau_o^c$ the central grains receive thermal radiation from a shell of grains somewhat cooler than the outer grains and $T_g(\tau_o)$ would be lower than our $T_{\lim}$, but still higher than $2{\cdot}7$°K. Such large values of τ_o are of course not likely to be of practical interest.

(d) *Variation of grain properties*

The results we have found for spherical grains of a single radius with optical ($\lambda \lesssim 10\mu$) properties constrained to approximate those observed for interstellar grains and with $Q_V \sim 1$, should apply also to a distribution of grain sizes or shapes subject to the same constraints. Results for types of grains other than those which we have explicitly considered, but satisfying the same constraints, can be estimated if their far infra-red efficiency lies in the range covered by the curves shown in Fig. 1. More quantitatively, we have found that even for $0{\cdot}15\mu$ graphite grains, which do not fit the observed extinction curves, T_g is different by no more than 10 per cent at any position within a cloud with $\tau_o = 30$ from the values found for $0{\cdot}05\mu$ graphite grains.

For grain models having $Q(\lambda) = e/\lambda$ throughout the far infra-red, where e is a constant determined by the grain properties, the relation between E_A, the energy absorbed per square centimetre of grain surface per second, and the grain temperature T_g is,

$$E_A = 1{\cdot}5 \times 10^{-4}\, eT^5 \text{ erg cm}^{-2}\text{-s}^{-1}. \tag{14}$$

Since E_A is determined chiefly by the optical properties of the grains, it will have similar values for all grain types which satisfy the constraints listed above (cf. Fig. 7), in the regions of the cloud where F_T and $F_{2.7}$ make small contributions. T_g for any such grain having $Q(\lambda) = e/\lambda$ can be obtained from our results for grains with impurity cooling ($\lambda_o = 100\mu$) by noting that if $Q_1(\lambda) = e_1/\lambda$, and $Q_2(\lambda) = e_2/\lambda$, then at corresponding positions within a cloud the temperatures of the two types of grains will be in the ratio

$$\frac{T_1(\tau, \tau_o)}{T_2(\tau, \tau_o)} = \left(\frac{e_2}{e_1}\right)^{1/5}. \tag{15}$$

Equation (15) is applicable so long as T_1 and $T_2 \gtrsim 4$°K, so that the greater part of the absorbed energy does not come from the microwave background.

We have not considered in this paper types of grains for which $Q(\lambda) \ll 1$ even in the near ultra-violet and visible. Such grains (or mixtures containing them) might produce a good fit to the optical observations. They might also have sufficiently high $Q(\lambda) \sim Q_V \ll 1$ in the far infra-red (resulting perhaps from impurities) to permit them to reach very low temperatures $T_{go} \sim T_{eq}$ even in free-space because of the flatness of $Q(\lambda)$. Hoyle & Wickramasinghe (1969) have recently proposed one such grain model (see Appendix B).

(e) *Other heating mechanisms*

We have considered heating of grains only by the absorption of radiant energy, which is the dominant process under almost all circumstances. Other processes which may contribute to heating the grains are (1) collisions with gas atoms, (2) heat of formation of molecules forming on the grain surfaces (Solomon &

Wickramasinghe 1969) and (3) heating by cosmic rays (Salpeter & Wickramasinghe 1969). The influence of those processes on the physical conditions in a dust cloud will be the subject of further study.

6. CONCLUSIONS

The main results of this paper are contained in Figs 3–6 which give the grain temperature T_g as a function of position within spherical dust clouds of various total opacity. Our results reveal some qualitative effects which should be independent of the exact nature of interstellar grains. We have found that the infra-red component of the near interstellar radiation field penetrates to the centre of clouds of high visual opacity τ_0 and prevents the grain temperature from falling sharply. As τ_0 rises, and this radiation is excluded, the central grains assume a limiting temperature owing to the thermal radiation from the grains in the cloud exterior. The temperature falls below this limiting temperature only for clouds of exceedingly high τ_0.

We have explored the effects of enhancement of the far infra-red emissivity by impurity oscillators. The influence of such oscillators on the grain temperatures and on the temperature profiles of clouds depends separately on the strength and the frequency spectrum of the oscillators. It is, therefore, necessary to specify these quantities in detail when studying impurity effects. For grains with visual extinction efficiency $Q_V \sim 1$, we have found that even the maximum amount of impurity cooling predicted by a simple theoretical argument is not sufficient to reduce grain temperature below $\sim 5\,^\circ$K in dust clouds of the maximum range of opacity ($\tau \sim 5$ mag) which has been observed in the Galaxy. This suggests that it may not be possible in typical regions of the galactic plane to cool such grains sufficiently to permit formation of solid H_2 mantles. Only grains with $Q_V \ll 1$ might attain sufficiently low temperatures, as discussed in Section 5d. On the other hand, it is unlikely that the high temperatures ($\sim 40\,^\circ$K) predicted for pure graphite grains are attained in practice, since even a small addition of impurity oscillators (or a thin mantle), reduces the temperature somewhat (see Fig. 6).

Although we have considered explicitly only spherical dust clouds, our results are easily generalized to other geometries. Similarly, the results can be applied to a greater variety of grain models than explicitly considered. Accurate temperatures for any grains having $Q(\lambda) \propto 1/\lambda$ in the far infra-red, e.g. dielectric grains and grains with impurities may easily be obtained (see Section 5d). Estimates are also possible for grains with other types of far infra-red absorption efficiency.

Our results indicate that T_g may vary by less than a factor of three from free-space to the centres of the most opaque clouds, and that for most grain types the variation is by less than a factor of two to the centre of clouds with $\tau_0 \sim 5$ (see Figs 5a and 6a). We have also found that the free-space grain temperature varies very slowly as the starlight radiation field is changed. The resulting expected small variation of T_g with position indicates that a single direct or indirect measurement of the value of T_g in any region of space would be extremely useful.

We have been concerned throughout only with static equilibrium configurations and not at all with the evolution of dust clouds. The evolution must depend on the gas temperature, which in turn is related in a complicated fashion to the grain temperature T_g. It is hoped that our detailed results for T_g can be applied in studies of the evolutionary problem.

ACKNOWLEDGMENTS

We wish to thank Dr N. C. Wickramasinghe for assistance in calculating the grain properties, and Dr K. S. Krishna Swamy for providing the properties of the core-mantle grains. We thank Drs D. W. Stibbs, H. C. van de Hulst, J. M. Greenberg and N. C. Wickramasinghe for helpful discussions.

Michael W. Werner:
Department of Physics, University of California, Berkeley, California.

E. E. Salpeter:
Department of Physics, Cornell University, Ithaca, New York.

REFERENCES

Abramowitz, M. & Stegun, I., 1964. *Handbook of Mathematical Functions*, National Bureau of Standards, Washington, D.C.
Bertie, J. G. & Whalley, E., 1967. *J. chem. Phys.*, **46,** 1271.
Donn, B. & Krishna Swamy, K. S., 1969. *Physica*, **41,** 144.
Field, G. B., 1969. *Mon. Not. R. astr. Soc.*, **144,** 411.
Field, G. B., Partridge, R. B. & Sobel, H., 1967. In *Interstellar Grains*, eds J. M. Greenberg & T. P. Roark, NASA publication SP–140, Washington, D. C.
Greenberg, J. M., 1968. *Stars and Stellar Systems*, **7,** 221.
Habing, H. J., 1968. *Bull. astr. Inst. Netherl.*, **19,** 421.
Heiles, C. E., 1968. *Astrophys. J.*, **151,** 919.
Hoffmann, W. F. & Frederick, C. L., 1969. *Astrophys. J.*, **155,** L9.
Hoyle, F. & Wickramasinghe, N. C., 1962. *Mon. Not. R. astr. Soc.*, **124,** 417.
Hoyle, F. & Wickramasinghe, N. C., 1967. *Nature*, **214,** 969.
Hoyle, F. & Wickramasinghe, N. C., 1969. *Nature*, **223,** 459.
Irvine, W. M. & Pollack, J. B., 1968. *Icarus*, **8,** 324.
Krishna Swamy, K. S. & Wickramasinghe, N. C., 1968. *Mon. Not. R. astr. Soc.*, **139,** 283.
Lambrecht, H. & Zimmermann, H., 1954. *Mitteil. Univ.-Sternw. Jena*, Nr. 13.
Lillie, C. F., 1968. Ph.D. Thesis, University of Wisconsin; paper presented at 128th AAS meeting, Austin, Texas.
Salpeter, E. E. & Wickramasinghe, N. C., 1969. *Nature*, **222,** 442.
Solomon, P. M. & Wickramasinghe, N. C., 1969. *Astrophys. J.*, **158,** in press.
Taft, E. A. & Phillipp, H. R., 1965. *Phys. Rev.*, **138A,** 197.
Van de Hulst, H. C., 1957. *Light Scattering by Small Particles*, Chapmen and Hall, London.
Van de Hulst, H. C. & Irvine, W. M., 1963. *Mem. Soc. Roy. Sci. Liege*, **7,** 78.
Wickramasinghe, N. C., 1967. *Interstellar Grains*, Chapman and Hall, London.
Wickramasinghe, N. C. & Reddish, V. C., 1968. *Nature*, **218,** 661.

MATHEMATICAL APPENDIX A

Consider a semi-infinite medium with a plane boundary, illuminated from the outside by isotropic radiation. Assume a uniform distribution of absorbers and scatterers throughout the medium with albedo γ (ratio of scattering to total extinction). Let x be the total extinction optical depth at a point in the medium, measured to the nearest point on the surface. We wish to calculate $F_T(x)$, the flux averaged over direction of direct and scattered radiation at x, by the method of successive scatterings (van de Hulst & Irvine 1963)

Let $F_n(x)$ be the averaged (over direction) flux of n-times scattered light at depth x. A slab of thickness dy at y then makes a contribution to $F_{n+1}(x)$ of

$$dF_{n+1}(x) = \gamma dy F_n(y) \int_0^1 d|\mu| \, |\mu|^{-1} \exp\left(-|x-y|/|\mu|\right). \qquad \text{(A1)}$$

We can then express $F_T(x)$ in terms of a power series in γ,

$$F_T(x) = F_0(x)\left[1 + \sum_{n=1}^{\infty} \gamma^n f_n(x)\right], \tag{A2}$$

where

$$F_0(x)f_{n+1}(x) = \tfrac{1}{2}\int_0^{\infty} dy F_0(y)f_n(y)E_1(|x-y|), \tag{A3}$$

and E_1 is the first exponential integral. In these expressions F_0 is the unscattered (but attenuated) flux, which is obtained as

$$F_0(x) = \tfrac{1}{2}E_2(x) = \tfrac{1}{2}\{e^{-x} - xE_1(x)\} \tag{A4}$$

and $f_0 = 1$.

We have evaluated numerically successive integrals of the form of equation (A3), starting with $f_0 = 1$ and a polynomial approximation to E_1 (Abramowitz & Stegun 1964). The range of the integrand for small $|x-y|$ was dealt with separately using the identity

$$\int_{x_1}^{x_2} (a+bx)E_1(x)\,dx = [bE_3(x) - be^{-x} - aE_2(x)]_{x_1}^{x_2}. \tag{A5}$$

We carried out calculations for x up to 20 and n up to 7 and the values of f_n are given to better than 5 per cent by the polynomials in Table AI.

TABLE AI

Scattering polynomials

$$f_1 = (0{\cdot}25 + 1{\cdot}44x + 0{\cdot}045x^2)/(1 + 0{\cdot}6x + 0{\cdot}0001x^4)$$
$$f_2 = (0{\cdot}1240 + 0{\cdot}95x + 0{\cdot}025x^2)/(1 + 0{\cdot}11x)$$
$$f_3 = (0{\cdot}07726 + 1{\cdot}029x)$$
$$f_4 = (0{\cdot}05406 + 0{\cdot}580x + 0{\cdot}11x^2)/(1 + 0{\cdot}00056x^2)$$
$$f_5 = (0{\cdot}040 + 0{\cdot}3x + 0{\cdot}28x^2)/(1 + 0{\cdot}001x^2)$$
$$f_6 = (0{\cdot}032 + 0{\cdot}07x + 0{\cdot}42x^2)/(1 + 0{\cdot}00027x^2)$$
$$f_7 = (0{\cdot}025 - 0{\cdot}08x + 0{\cdot}46x^2 + 0{\cdot}011x^3)$$

For the approximate treatment of spherical geometry in Section 3 we argue as follows. Let x be the optical depth from any point in the sphere to the nearest point on the surface and x_0 the value of x at the centre. If $x_0 \gg 1$ then the results of the plane geometry case are accurately applicable except in the central region ($x \sim x_0$). In the opposite extreme of $x_0 \ll 1$, the singly scattered flux F_1 for the spherical case can be evaluated easily and multiple scattering is unimportant (even if $\gamma \to 1$). The ratio $F_1(0)/F_0(0)$ in this case is $\frac{1}{2}\gamma x_0$, whereas for the plane parallel case with albedo γ'' the ratio $f_1(0)$ is $0{\cdot}25\,\gamma''$. The singly scattered flux at the surface of the sphere is then given correctly by the plane parallel result if we make the substitution $\gamma \to 2x_0\gamma$. As a simple interpolation prescription for the flux at a depth x within a spherical cloud of radius x_0 we shall then use equation (A2) with the $\{f_n\}$ in Table AI, but with γ replaced by

$$\gamma' = \gamma(1 - e^{-2x_0}) \tag{A6}$$

for all x and all γ, and with F_0 calculated exactly for the spherical geometry. As described above, this prescription is accurate for all x only when $x_0 \gg 1$ and only for $x = 0$ when $x_0 \ll 1$, but it is still of the correct order of magnitude elsewhere.

APPENDIX B (added in proof)

TEMPERATURES OF LOW CONDUCTIVITY GRAINS

Hoyle & Wickramasinghe (1969) have argued that grains with low conductivity could have $Q(\lambda) \equiv Q(\lambda_0) \ll 1$ at all wavelengths below λ_0 in the far infra-red. For $\lambda > \lambda_0$, $Q(\lambda)$ would decrease as in equation (7) above. For large λ_0, such grains could attain very low temperatures even in free-space because of the flatness of $Q(\lambda)$. For grains of this general type it is possible that $Q(\lambda)$ may increase above $Q(\lambda_0)$ in the ultra-violet, so that the free-space temperatures would rise; however, within a cloud the grains temperatures would still be quite low.

We have calculated the temperatures for a grain of this type having appreciable absorption efficiency in the ultra-violet by taking the following values for $Q(\lambda)$:

$$Q(\lambda) = 1, \quad \lambda < \lambda_1$$

$$Q(\lambda) = 4\pi^2 a/\lambda_0, \quad \lambda_1 < \lambda < \lambda_0$$

$$Q(\lambda) = 4\pi^2 a/\lambda, \quad \lambda > \lambda_0.$$

We let $\lambda_0 = 750\ \mu$ and $a = 0{\cdot}15\ \mu$. The temperatures are shown in Table BI for several choices of λ_1, and for grains in free-space (T_{g0}) and at the centre of a cloud with $\tau_0 = 5$. $\lambda_1 = 0$ for grains with no ultra-violet absorption features. The results indicate that grains of this general type are capable of attaining very low temperatures within ordinary dust clouds, even if $Q(\lambda)$ is significant in the ultra-violet.

TABLE BI

Temperatures of low conductivity grains

λ_1:	0	0·15 μ	0·25 μ	0·35 μ
T_{g0}	3·7°K	4·65°K	6·45°K	7·55°K
$T(\tau = 5)$	3·35°K	3·4°K	3·4°K	3·4°K